

AD-A173 561

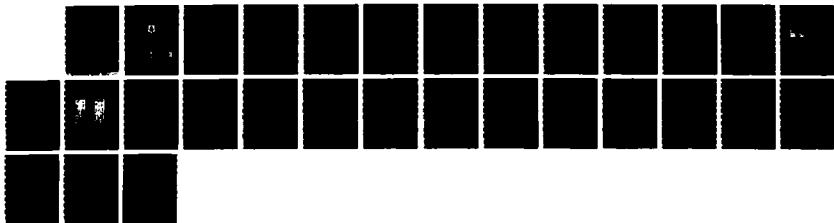
THE STUDY OF HEAT-SCAN INFRARED NDT TO THE INSPECTION
FOR ADHESION OF PRO (U) FOREIGN TECHNOLOGY DIV
WRIGHT-PATTERSON AFB OH 7 ENRUI ET AL 15 OCT 86
FTD-ID(RS)T-8722-86

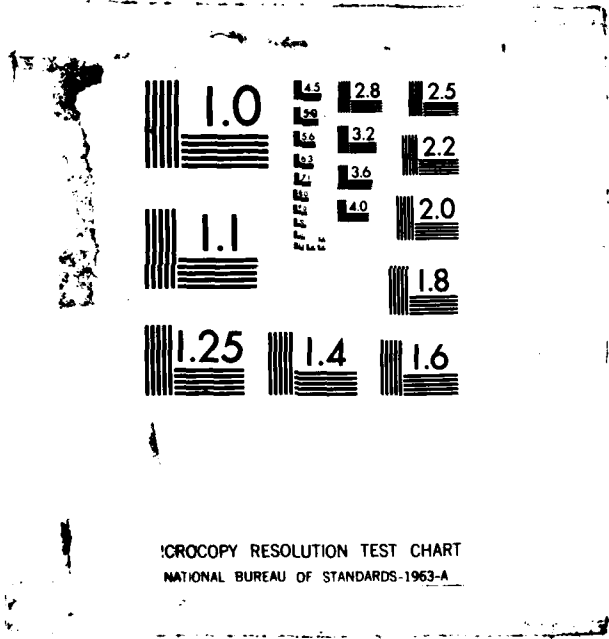
1/1

UNCLASSIFIED

F/G 14/2

NL





XEROCOPY RESOLUTION TEST CHART
NATIONAL BUREAU OF STANDARDS-1963-A

2

FTD-ID(RS)T-0722-86

AD-A173 561

FOREIGN TECHNOLOGY DIVISION



THE STUDY OF HEAT-SCAN INFRARED NDT TO THE INSPECTION FOR ADHESION OF PROPELLANT OF ROCKET MOTOR TO THE ENVELOPE

by

Tian Enrui, Wu Jie, Pi Miugjia

DTIC FILE COPY



DTIC
ELECTE
NOV 03 1986
S E D

Approved for public release;
Distribution unlimited.



86 11 3 087

HUMAN TRANSLATION

FTD-ID(RS)T-0722-86

15 Oct 86

MICROFICHE NR: FTD-86-C-002288

THE STUDY OF HEAT-SCAN INFRARED NDT TO THE INSPECTION FOR ADHESION OF PROPELLANT OF ROCKET MOTOR TO THE ENVELOPE

By: Tian Enrui, Wu Jie, Pi Miugjia

English pages: 24

Source: Harbin Gongye Daxue Xuebao, Vol. 3, Nr. 1, 1985, pp. 74-83

Country of origin: China

Translated by: FLS, INC.

F33657-85-D-2079

Requester: FTD/TQTA

Approved for public release; Distribution unlimited.

| | |
|--------------------|----------------------|
| Accession No. | |
| NTIS GRA&I | * |
| DTIC TAB | |
| Unannounced | |
| Justification | |
| By _____ | |
| Distribution/ | |
| Availability Codes | |
| Dist | Avail and/or Special |
| A-1 | |



| | |
|---|---|
| <p>THIS TRANSLATION IS A RENDITION OF THE ORIGINAL FOREIGN TEXT WITHOUT ANY ANALYTICAL OR EDITORIAL COMMENT. STATEMENTS OR THEORIES ADVOCATED OR IMPLIED ARE THOSE OF THE SOURCE AND DO NOT NECESSARILY REFLECT THE POSITION OR OPINION OF THE FOREIGN TECHNOLOGY DIVISION.</p> | <p>PREPARED BY: TRANSLATION DIVISION FOREIGN TECHNOLOGY DIVISION WPAFB, OHIO.</p> |
|---|---|

GRAPHICS DISCLAIMER

All figures, graphics, tables, equations, etc. merged into this translation were extracted from the best quality copy available.

THE STUDY OF HEAT-SCAN INFRARED NDT TO THE INSPECTION FOR ADHESION
OF PROPELLANT OF ROCKET MOTOR TO THE ENVELOPE

Tian Enrui, Wu Jie and Pi Miugjia
Physics Teaching and Research Room

Submitted 10 July 1983

↘ This paper briefly describes the basic principles of the heat-scan infrared NDT and introduces the method and results of the utilization of Type HT-1 Heat-scan Infrared NDT Machine to the inspection for adhesion of the solid propellant of the rocket motor to the envelope. The selection of inspection parameters and the relations among them are analyzed and discussed, and the methods for defect signal recognition, defect location and semi-quantitative computations are proposed herein. This method can conveniently and rapidly evaluate the quality conditions of the adhesion of propellant to the envelope and has a guiding significance for the technology of propellant production.
↑

I. Preface

The existence of a defect such as adhesion separation of the solid propellant of a rocket motor from the envelope has seriously affected the use and finalization for production of solid propellant rocket motors. If ordinary inspection methods such as radiation, ultrasound, vortex, magnetic powder,etc. are used to test for this kind of defect, then either due to the method itself or certain limitations on its scope of application, it is difficult to satisfy the demands of inspection for quality of the adhesion of the propellant to the envelope. Therefore, in recent years, people have been actively researching the application of new technologies such as laser full-out, heat-scan infrared, etc. to solve the testing problem of the quality of the adhesion of the propellant to the envelope. Using the heat-scan infrared NDT to conduct inspection defects of the propellant at the envelope cannot only accurately determine defect location and estimate the size of the defect area, but also has advantages such as semi-automatic testing, permanent records, good repetitiveness, easy defect recognition, etc. Actual testings have proven that this is a better inspection method.

II. Theoretical Analysis

The key to using the infrared technology to conduct NDT inspection of an object is that there must be heat flow in the object and that the surface temperature distribution of the object must be obtained. The conduction of heat flow with a fixed intensity inside an object is closely related to the characteristics of thermal conduc-

tion of the object.

For an object with a fixed shape, there will be characteristic temperature distribution appearing on the surface of the object after a steady heat flow is input to the body; if there are defects inside the object, then since there is difference between the thermal characteristics of the part with the defect and those of the part without the defect, there will be temperature disturbance at the location of the defect, and thus there will be certain changes in the temperature distribution appearing on the surface of the object. Therefore, infrared NDT inspection is a method which, through infrared radiation on the surface of the object to be tested, obtains the temperature distribution on the surface of the object, then in turn inspects whether there are defects inside the object based on the temperature distribution.

There are two kinds of methods, the constant temperature and the instantaneous heat-scan, which inspect defects through temperature measurements of an object that has heat flow generated inside. This paper only analyzes the heat-scan method.

1. Heat-Scan and the Temperature distribution on the Surface of an Object

Heat-scan is using a point thermal radiation heat source with a constant radiation intensity to heat the surface of the object to be inspected by scanning at a constant speed, and then using an infrared sensor which is at a fixed location relative to the point

radiation heat source and is synchronized with the heat source temperature of the object, thereby obtaining the surface temperature distribution of the object.

Assume the object to be tested is set in the stationary coordinate system (x, y, z) , and the point radiation heat source with constant intensity and the sensor are set in the moving coordinate system (ξ, y, z) . The moving coordinate system is moving at a constant speed in the x -direction relative to the stationary coordinate system as shown in Fig. 1.

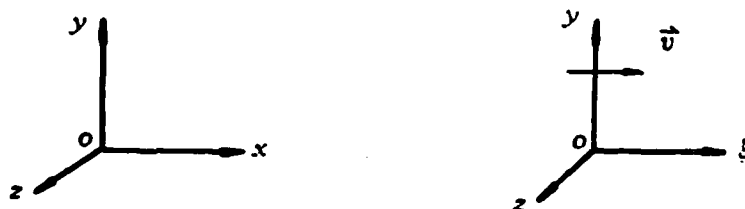


Fig. 1. Diagram of coordinate systems conversion

In the stationary coordinate system (x, y, z) , the thermal conduction equation inside the object is:

$$\frac{\partial^2 T}{\partial x^2} + \frac{\partial^2 T}{\partial y^2} + \frac{\partial^2 T}{\partial z^2} = \frac{1}{a} \frac{\partial T}{\partial t} \quad (1)$$

where T is the absolute temperature, $a = \frac{k}{\rho c}$ is the thermal diffusion coefficient, ρ is the density of the object, c is the specific heat of the object, k is the thermal conductivity of the object and t is time. It can be seen from Equation (1) that temperature T is a function of space and time, that is

$$T = T(x, y, z, t) \quad (2)$$

In the moving coordinate system (ξ, y, z) , since $\xi = x - vt$, Equation (1) can be changed to:

$$\frac{\partial^2 T}{\partial \xi^2} + \frac{\partial^2 T}{\partial y^2} + \frac{\partial^2 T}{\partial z^2} = -\frac{v}{a} \frac{\partial T}{\partial \xi} \quad (3)$$

When the object is a uniform board with semi-infinite thickness, the solution of Equation (3) is: [1] [2]

$$T = T_0 + \frac{q_0}{2\sqrt{\pi k r}} e^{-\frac{v}{2a}\xi} \cdot e^{-r\left[\left(\frac{v}{2a}\right)^2 + \frac{h}{k}\right]^{1/2}} \quad (4)$$

where $r = (\xi^2 + y^2 + z^2)^{1/2}$, the location of a point inside the object

T is the object surface temperature after heating

T_0 is the object surface temperature before heating

q_0 is the heat flow input to the surface of the object (heat input rate)

h is the surface heat exchange coefficient including thermal radiation and air natural convection.

It can be seen from Equation (4) that: in the coordinate system (ξ, y, z) of the heat source and the sensor, the temperature distribution on the surface of the object is independent to time t . Obviously,

$$T = T(q_0, k, a, v, r, h) \quad (5)$$

Thus, the surface temperature distribution of the object measured by the sensor does not change with respect to time. That is, there is a quasi-steady temperature distribution in the moving coordinate system.

It can be shown from Equations (4) and (5) that there are three kinds of parameters which will affect surface temperature of the object: (1) geometric parameter r , which represents the geometric location of the testing point; (2) physical parameters α and k , which reflect the physical properties of the object material; (3) testing parameters q_0 , v , and h , which reflect the testing conditions.

When q_0 , r and h are constant, it can be shown from Equations (4) and (5) that: for an uniform and defect-free object material, since the value of parameters α and k are equal everywhere, the measured object surface temperature T at different locations will be constant when using the sensor to scan the surface of the object, i.e., no change in object surface temperature can be detected. Then,

$$\Delta T = 0 \quad (6)$$

For object material with defects (or nonuniform), since the physical properties (α , k) are different for parts with and without defects, there must be temperature disturbance generated at locations where there are defects. Assume the measured temperature at the location with defect is T' , then obviously

$$\Delta T = T' - T \neq 0 \quad (7)$$

It can be seen from the above analysis that when using the heat-scan method to measure the surface temperature distribution of the object, if the testing environment is identical and the input heat flow q_0 and the scanning speed v are constant, then the sensor cannot detect any changes in the temperature at various points on the object surface during the testing process for an uniform object without

defects. For an object with defects, however, since its thermal parameters α and k change, the sensor can detect differences in temperature on the object surface. Consequently, we can conduct defect detection for objects through the inspection of temperature distribution on its surface. When temperature disturbances on an object surface is detected, it can be determined that there are defects in the object (or nonuniformity). This is the theoretical basis for conducting defect detection using the heat-scan method.

2. The Infrared Radiation on the Object Surface and Inspection

The Plank's formula for black body is

$$e_{\lambda}(T) = \frac{2\pi hc^2}{\lambda^5} \frac{1}{e^{hc/\lambda kT} - 1} \quad (8)$$

where h is the Plank's constant, k is the Boltzmann constant, c is the speed of light in vacuum, $e_{\lambda}(T)$ is the radiancy of black body radiation. It can be obtained from Equation (8) that: the total radiancy of a black body is:

$$E(T) = \sigma T^4 \quad (9)$$

That is, the total radiancy $E(T)$ of a black body is proportional to the temperature T to the fourth power, where

$\sigma = 5.669606 \times 10^{-8} \text{ W} \cdot \text{m}^{-2} \cdot \text{K}^{-4}$, which is the Stefan-Boltzmann constant.

For a non-black body, it is

$$E(T) = \epsilon \sigma T^4 \quad (10)$$

where ϵ is the specific emissivity and is related to factors such as material property, surface condition, temperature, wavelength,

etc.

Similarly, from Equation (8) the Wayne's shift law can be obtained:

$$\lambda_m = \frac{b}{T} \quad (11)$$

That is, the maximum wavelength λ_m shifts toward short wave direction as temperature T increases. In the formula, $b=2.897 \times 10^{-3} \text{ m} \cdot \text{K}$. For ordinary object under $300 \sim 400 \text{ K}$, there will be radiation with maximum wavelength of $8 \sim 14 \mu\text{m}$ radiated from its surface.

Therefore, an infrared radiometer which responds to a fixed wavelength range can be adopted to detect infrared radiation on the surface of an object, i.e., to measure the surface temperature distribution of the object. This is the principle of infrared radiation inspection.

III. Testing Results

The type HT-1 Infrared NDT Machine manufactured by our institute is used as the inspection device. Figure 2 is a photographic picture of the machine. Figure 3 is the principle diagram of the type HT-1 Machine. The mechanical scanning device is controlled by the scanning driver circuit to make the propellant to be tested and the paper recording cylinder turn synchronously at a uniform speed. In the meantime, the heat source (infrared converging lamp), the infrared sensor and the recording pen are all made to move along the propellant axial direction at an uniform speed thereby realizing synchronized

spiral scan-heating by the heat input source and spiral scan-detection by the sensor. The signals obtained from the sensor are fed into the signal processing circuit to drive the recording pen and the temperature distribution on the surface of the propellant is recorded synchronously on the cylindrical recorder. The type HT-1 machine can automatically complete the entire process.

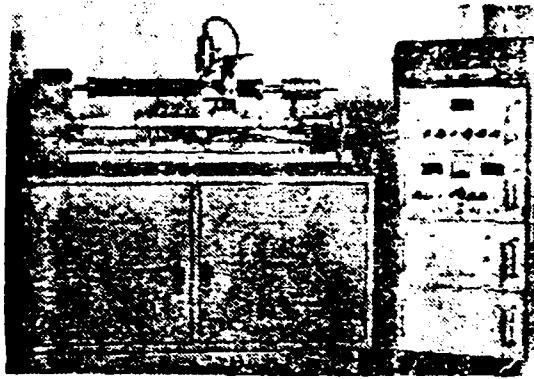


Fig. 2. Photograph of HT-1 Machine

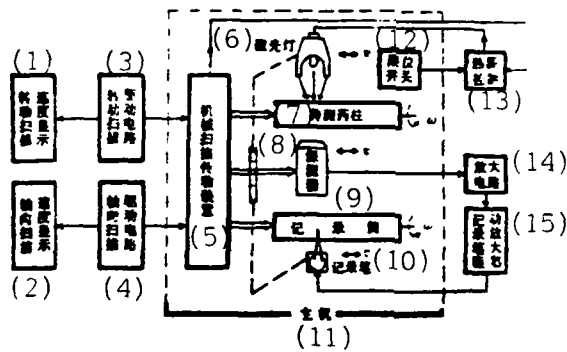


Fig. 3. The principle diagram of the HT-1 Machine

Key: (1) rotational scanning speed display; (2) directional scanning speed display; (3) rotational scanning driver circuit; (4) directional scanning driver circuit; (5) mechanical scanning transmission device; (6) converging lamp; (7) Propellant to be tested; (8) sensor; (9) recording cylinder; (10) recording pen; (11) main portion of machine; (12) switch; (13) heat source control; (14) amplification circuit; (15) driver amplifier of the recording pen.

The sample propellants tested were all provided by the propellant producing plant. Examples of testing results are as follows:

Propellant I: No. 2 propellant provided by the OOS plant, envelope thickness was 1.4 mm (hard) with smooth surface. There were man-made adhesion separation flaws of 7x7 mm², 6x6 mm², 10x10 mm² and 15x15 mm². It was mounted on the HT-1 machine for testing.

Testing parameters: voltage of the converging lamp was 5 volts. The diameter of the converging focus light spot was ϕ 6 mm; the scanning speed: rpm=16 revolution/min, horizontal moving speed=25 mm/min; the distance (axial) between the centers of the converging lamp and sensor=16 mm; room temperature was 24°C.

Testing results: See Fig. 4 for the heat-scan diagram. The results of diagram evaluation have already been indicated on Fig. 4. There were 5 defects. Results of the propellant autopsy: The locations and sizes of the defect are in total agreement with actuality. It is consistent with the records and the analysis of flaws recognition.

Propellant II: No. 2 propellant provided by the OOS plant, envelope thickness was 0.8 mm (soft) with smooth surface, yet certain local areas were not very smooth. There were natural adhesion separation flaws, unknown.

Testing parameters: voltage of the converging lamp was 6 volts. The diameter of the converging focus light spot was $\phi 6$ mm; the scanning speed: rpm=15 revolution/min, horizontal moving speed=30 cm/min; the distance between the centers of the converging lamp and sensor=16 mm; room temperature was 9°C.

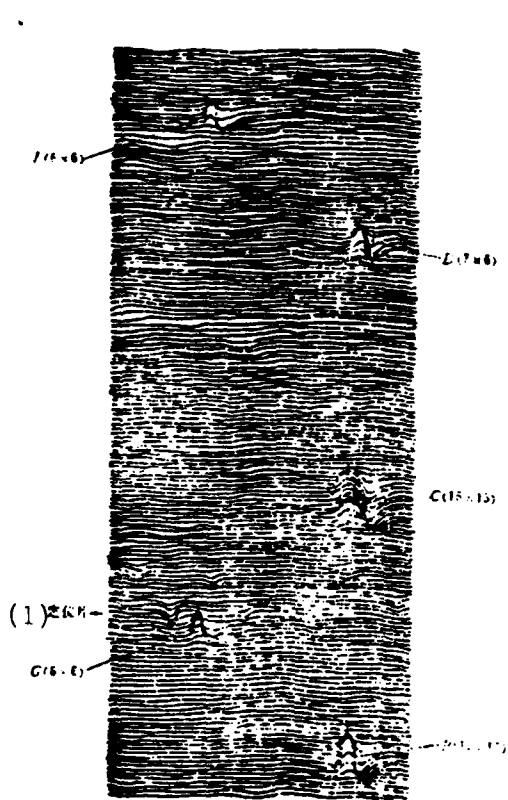


Fig. 4.
Key: (1) Location setter

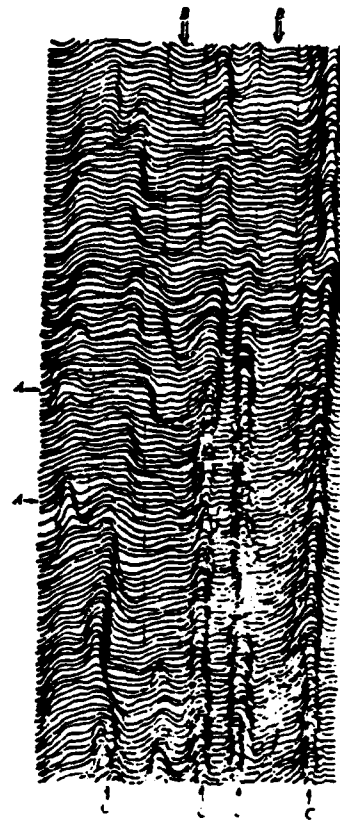


Fig. 5.

See Fig. 5 for the heat-scan diagram.

(1) Analytical evaluation of the scanning diagram: the envelope condition of the propellant had local adhesion separation A, large area adhesion separation B and strong adhesion area C.

(2) Results of propellant anatomy: There were numerous kinds of natural defects and were very irregular, which more truthfully reflects the actual production condition. The anatomical results are in agreement with the flaw analysis of the scanning record.

IV. Analysis and Selection of Testing Parameters

1. Amount of Heat Input and Heat Spots

The infrared converging lamp is used as heat input source for testing. The light (infrared and visible) emitted from the bromine-tungsten lamp is focused on the propellant by a gold-plated, elliptical cover. The radiation intensity of the light source is determined by the voltage of the lamp, which is generally kept under 10 volts. The diameter of the light spot is kept at about $\sqrt{6}$ mm.

The selection of the amount of heat input is primarily determined by the radiation intensity and scanning speed of the light source. If the radiation intensity of the light source is large (i.e., the corresponding lamp voltage is high) and scanning speed is low, the amount of heat input is large, and vice versa. Too large a heat input and a larger heat spot (light spot) will result in a greater temperature rise on the propellant surface and cause temperature interference between adjacent scanning lines and the temperature of the entire propellant to rise, thereby affecting the accuracy of testing. However, too low a heat input will decrease the temperature gradient at parts with defects, which is also bad for testing. Too small a heat spot will also cause detection sensitivity to drop

significantly. Therefore, they should be matched properly.

It can be shown from the relationship curves (Figs. 6, 7) of the instantaneous temperature at propellant envelope and the scanning speed under different lamp voltages that: when lamp voltage is smaller than 10 volts, at a properly selected scanning speed v the temperature at the surface between the propellant and the envelope can be kept under 25°C and the temperature on the outer surface of the envelope under 50°C . The testing is safe.

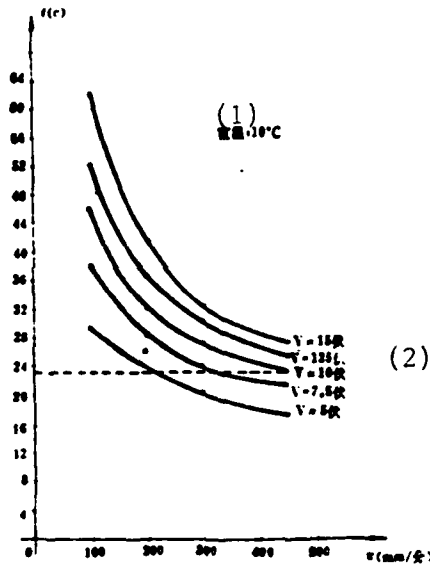


Fig. 6. No. 2 propellant envelope inner surface $t \sim v$ relationship curves
Key: (1) Room temperature: 10°C ;
(2) volt.

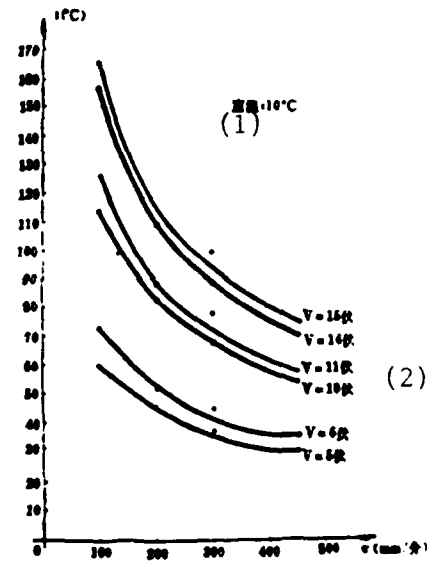


Fig. 7. No. 2 propellant outer surface $t \sim v$ relationship curves
Key: (1) Room temperature: 10°C ;
(2) volt.

It can be shown from the above analysis that the amount of heat input to the propellant surface is related to scanning speed, therefore it must be properly selected.

2. Scanning Velocity

The propellant rotates around its axis at a constant speed; the heat input source (converging lamp) and the sensor move along the axis of propellant at a constant velocity thereby resulting in the scanning of the propellant surface along a spiral line by the heat source and the sensor. The scanning velocity \vec{v} at a certain point on the propellant surface is the vector summation of the linear velocity \vec{v}_1 of the rotating line on the propellant surface and the heat source sensor velocity \vec{v}_2 along the axial direction, i.e.,

$$\vec{v} = \vec{v}_1 + \vec{v}_2$$

For the testing of No. 2 propellant, the axial moving speed v_2 is generally selected as $v_2 = 24$ mm/min. As the propellant turns, the linear speed v_1 of a certain point on its surface is 2400 mm/min. Thus, the value of the scanning speed is:

$$v = \sqrt{v_1^2 + v_2^2}$$

Since $v_2 \ll v_1$, $v \approx v_1 = 2400$ mm/min, i.e., the linear speed of a certain point on the propellant surface can be treated as the heat scanning speed. At this time, the pitch of the scanning line along the propellant surface is 2mm.

3. Time Lag

The time lag is the time required to detect the temperature at a certain point on the propellant surface after heat flow is input to that point, or simply called testing time lag. The time

lag is determined by the relative position between the focus point (i.e., heat input point) of the converging lamp and the sensing point of the sensor, and the scanning speed. When the rotational linear speed at a certain point on the propellant surface is much larger than the moving speed of the converging lamp and the sensor, the time lag Δt is approximately equal to the axial distance L between the centers of the converging lamp and sensor divided by the moving speed v_2 , i.e.,

$$\Delta t = \frac{L}{v_2} \quad (12)$$

Figure 8 is the $\Delta T \sim \Delta t$ relationship curves obtained from testing of 4 different adhesion separation defects at the envelope of No. 2 propellant. The Y-axis represents corresponding surface temperature difference ΔT of the parts with and without defects and the abscissa represents the testing time lag Δt . It can be seen from the figure that for every defect there is an optimum testing time lag Δt_{opi} and the temperature difference detected at this time will be a maximum, thus the highest testing sensitivity. Therefore, the testing time lag should be selected as close to the optimum time lag as possible during testing in order to obtain the highest testing sensitivity. Meanwhile, we also see that when there are defects of different sizes on the propellant surface, the testing time lag must be properly selected so that each defect can obtain a higher testing sensitivity under the same testing condition.

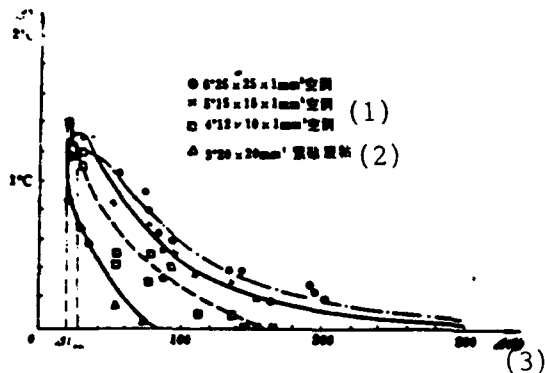


Fig. 8. Defect heat-scan infrared testing $\Delta T \sim \Delta t$ of sample 620-2. Key: (1) hole; (2) closely attached adhesion separation; (3) second.

For No. 2 propellant, the voltage of the converging lamp is generally selected as 6 volts; the rpm of the propellant is 12 revolutions/min; axial moving speed of the converging lamp and the sensor is 24 mm/min; the axial distance between the centers of the lamp and sensor is 16 mm. Then from Formula (12), the testing time lag is 40 seconds.

4. Surface Condition of the Propellant

It can be seen from Formula (10) that if the specific radio-activity ϵ at various points on the propellant surface is different, then under the same temperature there will be different radiation energy at various points on the propellant surface. Thus, there can be "bogus defect" signals which are similar to a defect signal and they become the source of radiation noise. Weaker defect signals are very easily drowned by this kind of "noise" and this creates difficulties in analyzing defects from the heat-scan diagrams.

Therefore, the condition of the propellant surface must be carefully observe before testing and proper records should be make. Efforts should be expended to make the specific radioactivity on the propellant surface uniform for the benefit of analyzing defects.

V. Recognition of Defect Signals and Determination of Locations and Sizes

1. Recognition of Defect Signals and Determination of Locations

The information recorded on the temperature distribution diagram is the infrared radiation of the propellant surface and every information is related to the internal heat characteristics of the propellant. In order to recognize flaws, the corresponding relationship between the infrared radiation information (i.e., propellant surface temperature distribution) of the propellant surface and the internal physical conditions of the propellant must be determined. The establishment of this relationship is based on a large number of experiments and anatomical verifications.

For the No. 2 propellant, since the envelope thickness changes abruptly at the head retention ring and the tail groove, there are distinctive characteristics in the corresponding temperature distribution signals. They are very easy to recognize and do not require special explanation. If there is no defect between the propellant and the envelope, the measured propellant surface temperature between the space of the heat source and the sensor will be uniform everywhere and the temperature distribution curve will be

straight lines without defect signals. If there are defects between the propellant and the envelope, there will be disturbance signals on the temperature distribution curves. In order to explain properly, the defects are generally classified into two types, based on their heat conduction characteristics:

(1) Heat resistance type defect: i.e., the heat conduction rate at the place with the defect is smaller than at the place without defect; in other words, the heat resistance at the place with the defect is larger. For instance, envelope adhesion separation, lamination, air bubble, etc. to name a few.

(2) Heat conduction type defect: i.e., the heat conduction rate at the place with defect is larger than that at the place without defect; in other words, the heat resistance at the place with defect is smaller. For instance, metallic or nonmetallic impurities, etc. with larger heat conductivities at the envelope.

Figure 9 (a) is a schematic diagram of defects at the propellant envelope. There is a heat resistance type defect at A, a heat conduction type defect at B and no defects in other places. The temperature distribution is as shown in Fig. 9 (b) when conducting heat-scan testing along the scanning line in the figure. The temperature increases at A, decreases at B and remains constant at other places. Since the signals underwent microprocessing in the testing system, the actual testing signals are as shown in Fig. 9 (c).

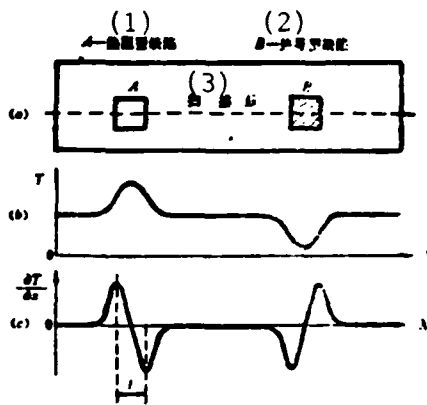


Fig. 9.

(a) Schematic diagram of defects at propellant envelope

(b) Temperature infrared distribution curve of testing

(c) Temperature gradient distribution curve

Key: (1) A-heat resistance type defect; (2) B-heat conduction type defect; (3) scanning line.

Actually since the shape and size of defects are all different, the measured testing signals are somewhat different from the typical curve shown in Fig. 9 (c) and they must be carefully recognized in actual testings.

There is a cylindrical recording device installed on the type HT-1 infrared NDT machine. The cylinder rotates synchronously with the propellant and its diameter is 1/2 of or equal to that of the propellant. The recording paper is wrapped around the cylinder. The electromagnetic type recording pen and the sensor move synchronously along the propellant axes, thus the recording pen will record synchronously on the recording paper the propellant surface temperature distribution scan-measured by the sensor. The propellant surface temperature distribution diagram corresponds to the propellant surface spread-out diagram. The axial ratio of correspondence is 1:1 and the circumferential ratio of correspondence is 1:2 or 1:1. The

locations of defect can be accurately determined based on these ratios.

2. Determination of the Size of Defect

It can be seen from the above analysis that the shape of the defect signal on the heat-scan diagram is a S-shape curve (or reversed S-shape). Since the shape and size of the defect are complex and irregular, the area of defect can only be approximately estimated by using, based on the temperature distribution diagram, the rectangular area method. If the geometric dimension of the defect in the axial direction is represented by a and that in the circumferential direction by b , the area of defect is:

$$S=a \cdot b \quad (13)$$

(1) Determination of the Geometric Dimension a of the Defect in the Axial Direction

Since the axial ratio of the heat-scan infrared testing diagram is 1:1, and if the number of recorded defect signal curve in the axial direction is n and pitch between the lines is h , the axial dimension of the defect is:

$$a=k_1 \cdot nh \quad (14)$$

where k_1 is the correction coefficient and is generally selected as $k_1=0.90$.

(2) Determination of Geometric dimension b of the Defect in the Circumferential Direction

Since the heat conductivity k changes abruptly at the interface between a defect and its surroundings, it has been verified through theoretical analysis that the point of maximum temperature gradient change on the temperature distribution curve is at the interface between the defect and its surroundings. Therefore, the geometric dimension b of the defect in the circumferential direction should be the distance l (Fig. 9 (c)) between the two peaks of the reversed S-shaped curve. The circumferential ratio of the heat-scan testing diagram is known as 1:2, then:

$$b = k_2 \cdot 2l \quad (15)$$

where k_2 is the correction coefficient in the circumferential direction. The area of defect can be obtained by substituting Formulae (14) and (15) into Formula (13)

$$S = G(nh) \cdot 2l \quad (16)$$

where $G = k_1 \cdot k_2$ and it is generally selected as $G = 0.8 \sim 0.9$.

In Fig. 4 of the heat-scan diagram for No. 2 propellant, for example, the number n of the scanning line of defect signal found at I is equal to 4 and the pitch h between the lines is equal to 1.6. The distance h between the two peaks on the defect signal is equal to 3, then the area of the defect is

$$\begin{aligned} S = a \cdot b &= G(nh)(2l) = 0.9(4 \times 1.6)(2 \times 3) \\ &= 0.9(6.4)(6) \doteq 35 \text{ mm}^2 \end{aligned}$$

The area of defect S at I was found to be equal to $6 \times 6 = 36 \text{ mm}^2$ after anatomical measurement. This is in basic agreement with the calculated

result.

VI. Conclusions

Using the Type HT-1 Infrared NDT Machine, which adopts the heat-scan infrared NDT technology, to conduct inspection for adhesion separation of certain propellants of rocket motors from the envelope is an effective method. It has advantages such as simple equipment, convenient operation, safety and reliability, high sensitivity, semi-automatic testing, direct recording, easy flaw recognition, accurate location determination, etc.

It is shown from the testing and anatomical results for No. 2 propellant that the types of defect detected include adhesion separation (including natural and man-made adhesion separation), air bubble, nonuniform glue spreading or nonuniform envelope thickness, etc. between the propellant and the envelope. The smallest size of defect detected was $5 \times 5 \text{ mm}^2$.

Since the shape and size of defect are related to the property and condition of the defect, the recognition of defect flaws requires further accumulation of experience and establishment of flaw recognition standards.

Our gratitude: Professor Hong Jing took the time to review this paper between his busy schedules and proposed valuable opinions. We hereby express our deepest appreciation.

REFERENCES

- [1] AD299230.
- [2] Arnold W. Schultz, *An Analytical Approach to Infrared Nondestruction Testing U.S.A.* 19.

The Study of Heat-Scan Infrared NDT to the Inspection for Adhesion of Propellant of Rocket Motor to Envelop

Tian Enrui Wu Jie Pi Mingjin

Abstract

This paper introduces basic principles of heat-scan infrared NDT and describes the method and the results of the applications of the Heat-scan Infrared NDT Machine Type HT-1 to the inspection for adhesion of the propellant of the rocket motor to the envelop. The selection of the testing parameters and the relations among them are analyzed and discussed. The methods of recognition, location and evaluation of the defect signal are proposed. This method can conveniently and rapidly evaluate the quality of the adhesion of the propellant to the envelop and has a guiding significance for the technology of propellant production.

DISTRIBUTION LIST
DISTRIBUTION DIRECT TO RECIPIENT

| <u>ORGANIZATION</u> | <u>MICROFICHE</u> |
|------------------------|-------------------|
| A205 DMAHTC | 1 |
| A210 DMAAC | 1 |
| B344 DIA/RTS-2C | 9 |
| C043 USAMIIA | 1 |
| C500 TRADOC | 1 |
| C509 BALLISTIC RES LAB | 1 |
| C510 R&T LABS/AVRADCOM | 1 |
| C513 ARRADCOM | 1 |
| C535 AVRADCOM/TSARCOM | 1 |
| C539 TRASANA | 1 |
| C591 FSTC | 4 |
| C619 MIA REDSTONE | 1 |
| D008 NISC | 1 |
| E053 HQ USAF/INET | 1 |
| E404 AEDC/DOF | 1 |
| E408 AFWL | 1 |
| E410 AD/IND | 1 |
| E429 SD/IND | 1 |
| P005 DOE/ISA/DDI | 1 |
| P050 CIA/OCR/ADD/SD | 2 |
| AFIT/LDE | 1 |
| FTD | |
| CCY | 1 |
| NLA/PHS | 1 |
| LLVL/Code L-389 | 1 |
| NASA/NST-44 | 1 |
| NSA/1213/TDL | 2 |
| ASD/FTD/1Q1A | 1 |

END

11-86

DTIC